International Journal of Ocean Engineering and Technology Vol. 6, No. 1, pp 51~59, December 2003 (ISSN 1225-0767)

Ultimate Strength Analysis of Ring-stiffened Cylinders with Initial Imperfections(I)

CHI-MO PARK* AND DONG-MIN PARK**
*School of Transportation Systems Engineering, University of Ulsan, Ulsan, Korea
**Hyundai Heavy Industry Co. Ltd., Ulsan, Korea

KEY WORDS: Ring-Stiffened Cylinders, Ultimate Strength, Initial Deformation, Initial Stress, Imperfection Sensitivity

ABSTRACT: *This paper has developed an efficient nonlinear finite element method that covers both initial deformations and initial stresses of general distribution in calculating the ultimate strength of ring-stiffened cylinders. The developed method and two widely-used commercial codes (NASTRAN and ABAQUS) were simultaneously applied to the same analysis model within the extent of those commercial codes' coverage to check the validity of the present method. After the validity check, it was used for parametric studies for more general cases of initial stress distribution, which produced some useful information about the imperfection sensitivity of the ultimate strength of ring-stiffened cylinders.*

1. Introduction

While ring-stiffened cylinders are very useful structural elements used in a submarine pressure hull or as members of offshore structures, research on the theoretical analysis of their ultimate strength has been very inactive and related structural designs have mainly depended on empirical formulas lacking theoretical background due to the following problems;

- One-dimensional (axisymmetric) finite element analysis is greatly computation-efficient, but has had a limited allowance of nonlinarities covering only geometrical nonlinearity and excluding material nonlinearity.
- Three-dimensional finite element analysis is not only computation-inefficient but also not fully developed to cover all types of initial imperfections, especially only having coverage of very simple distributions of initial stresses. (Park and Lee, 2001, 2002)

This paper offers a solution to these problems by improving the one-dimensional finite element method so that it can cover both geometrical and material nonlinearities and also all types of initial imperfections. In the conventional axisymmetrical analyses (Subbiah, 1988), circumferential integration in making the element stiffness matrix used to be carried out analytically, by which material nonlinearity could not be covered. Our present method has overcome this problem by adopting the following two concepts;

- Gauss quadrature to the circumferential direction as well as to the longitudinal direction
- layered approach to the thickness direction

This way, the distribution of material properties over a surface and through its thickness, which varies with the yielding process, can be properly taken into account and also the initial imperfections of any distribution can easily be considered by putting them as the initial condition of the solution procedure for a nonlinear problem. The developed method and two widely-used commercial codes (NASTRAN and ABAQUS) were simultaneously applied to an available test model, only considering initial deformations because these two commercial codes do not cover the general case of initial stress distributions, and their results are compared to one another to check the validity of the present method. After validation, it is applied to a series of models to perform parametric studies for the imperfection sensitivity of ultimate strength of ring-stiffened cylinders.

The first author : Chi-Mo Park
Email : cmpark@mail.ulsan.ac.kr

2. Elasto-Plastic Large Deformation Theory Of Circular Cylindrical Shells

2.1 Incremental strain-displacement relations

According to the theory of thin cylindrical shell, strain-displacement relations can be expressed as (Washizu, 1975; Brush and Almroth, 1975)

$$
\begin{aligned}
e_s &= u,_s + \frac{1}{2} w,_s{}^2 - z w,_{ss} \\
e_\theta &= \frac{1}{r}(v,_\theta + w) + \frac{1}{2r^2}(w,_\theta - v)^2 \\
&\quad - z\frac{1}{r^2}(w,_{\theta\theta} - v,_\theta) \\
\gamma_{s\theta} &= \frac{1}{r} u,_\theta + v,_s + \frac{1}{r} w,_s (w,_\theta - v) \\
&\quad - z\frac{2}{r}(w,_{s\theta} - \frac{1}{2} v,_s)
\end{aligned} \tag{1}
$$

where u, v and w are displacement components respectively to the axial(s), circumferential(θ) and radial(z) directions.(see Fig.1)

From eq. (1), the relations between strain increments and displacement increments can be obtained as follows.

$$
\begin{aligned}
\triangle e_s &= \triangle u,_s + w,_s \triangle w,_s - z \triangle w,_{ss} + \frac{1}{2}(\triangle w,_s)^2 \\
\triangle e_\theta &= \frac{1}{r}(\triangle v,_\theta + \triangle w) + \frac{1}{r^2}(w,_\theta - v)(\triangle w,_\theta - \triangle v) \\
&\quad - z\frac{1}{r^2}(\triangle w,_{\theta\theta} + \triangle v,_\theta) + \frac{1}{2r^2}(\triangle w,_\theta - \triangle v)^2 \\
\triangle \gamma_{s\theta} &= (\frac{1}{r}\triangle u,_\theta + \triangle v,_s) + \frac{1}{r}\{w,_s(\triangle w,_\theta - \triangle v) \\
&\quad + (w,_\theta - v)\triangle w,_s\} - z\frac{2}{r}(\triangle w,_{s\theta} - \frac{1}{2}\triangle v,_s) \\
&\quad + \frac{1}{r}\triangle w,_s(\triangle w,\theta - \triangle v)
\end{aligned} \tag{2}
$$

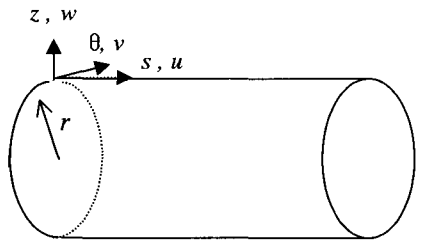

Fig. 1 Coordinate system of a circular cylindrical shell

Eq. (2) can be rewritten in a simplified form of a tensor equation divided into two parts; first- and second-order terms, as follows

$$
\triangle e_{ij} = \triangle \varepsilon_{ij} + \triangle e_{ij}{}^{(2)} \quad i,j = s, \theta \tag{3}
$$

The first-order term $\triangle \varepsilon_{ij}$ in eq. (3) can again be divided into three parts as

$$
\{\triangle \varepsilon\} = \{\triangle \varepsilon_m\} + \{\triangle \varepsilon_n\} + \{\triangle \varepsilon_b\} \tag{4}
$$

where $\{\triangle \varepsilon_m\}$ is a membrane strain term, $\{\triangle \varepsilon_n\}$ is a nonlinear term related to the total displacement of the current incremental stage and $\{\triangle \varepsilon_b\}$ is a bending strain term.

2.2 Incremental stress–strain relation

Incremental stress-strain relations are generally expressed as

$$
\{\triangle \sigma\} = [D]\{\triangle \varepsilon\} \tag{5}
$$

where $\{\triangle \sigma\} = [\triangle \sigma_s \ \triangle \sigma_\theta \ \triangle \tau_{s\theta}]^T$ and $[D]$ is an elastic coefficient matrix $[D_e]$ in the elastic range of material and as the stresses increase beyond the proportional limit it should be substituted by the elasto-plastic coefficient matrix $[D_{ep}]$ which can be obtained according to the flow theory of plasticity (Owen and Hinton, 1980).

2.3 Incremental virtual work equation with the follower force effect of hydrostatic pressure

Using the incremental theory based on the Lagrangian approach, the principle of virtual work (Washizu, 1975) is expressed as

$$
\int_v (\sigma_{ij} + \triangle \sigma_{ij}) \delta \triangle e_{ij} dv^o - \int_s (F_i + \triangle F_i) \delta \triangle u_i ds^o = 0 \tag{6}
$$

where dv^o and ds^o are, respectively, an elementary volume and an elementary surface area in the initial state, and afterwards they will be expressed as dv and ds for convenience and F_i refers to the external load components. In order to consider the follower force effect of hydrostatic pressure, the second term of eq. (6) can be written (Subbiah and Natarajan, 1982) as

$$
Q = -\int_s (F_i + \triangle F_i) \delta \triangle u_i ds = -\int_s (p + \triangle p) dA \cdot \delta \triangle U \tag{7}
$$

where p is the magnitude of hydrostatic pressure, dA is the infinitesimal area vector of which orientation keeps normal to the shell surface and of which magnitude is rdθds and $\delta \triangle U$ is a virtual incremental displacement vector $(\delta \triangle u, \delta \triangle v, \delta \triangle w)$.

After some manipulation (Park, 1990), eq. (7) becomes

$$
Q = -(p + \triangle p) \int_s \delta \{\triangle q\}^T \{d_f\} ds \tag{8}
$$

where $\{d_f\}$ can be divided into three parts: zero, first and second order terms, respectively as

$$\{d_{f0}\}=\begin{Bmatrix}0\\0\\r\end{Bmatrix},\quad \{d_{f1}\}=\begin{Bmatrix}-rw_{,s}\\-(w_{,\theta}-v)\\(v_{,\theta}+w+ru_{,s})\end{Bmatrix},$$

$$\{d_{f2}\}=\begin{Bmatrix}v_{,s}(w_{,\theta}-v)-w_{,s}(v_{,\theta}+w)\\w_{,s}\,u_{,\theta}-u_{,s}(w_{,\theta}-v)\\u_{,s}(v_{,\theta}+w)-v_{,s}\,u_{,\theta}\end{Bmatrix} \tag{9}$$

By putting eqs. (3), (5), (8) into eq. (6) and neglecting higher order terms, following incremental virtual work equation can be obtained in a matrix form.

$$\begin{aligned}&\int_{sh}\delta\{\triangle\varepsilon\}^T[D]\{\triangle\varepsilon\}dv+\int_{st}\delta\{\triangle\varepsilon\}^T[D]_{st}\{\triangle\varepsilon\}dv\\&+\int_{sh}\delta\{\triangle\phi\}^T[S_0]\{\triangle\phi\}dv+\int_{sh}\delta\{\triangle\phi\}^T[S_0]_{st}\{\triangle\phi\}dv\\&=\triangle p\int_s\delta\{\triangle q\}^T\{d_f\}ds-(\int_{sh}\delta\{\triangle\varepsilon\}^T\{\sigma\}dv\\&+\int_{st}\delta\{\triangle\varepsilon\}^T\{\sigma\}_{st}dv-p\int_s\delta\{\triangle q\}^T\{d_f\}ds)\end{aligned} \tag{10}$$

where

$$\{\triangle\phi\}=[\triangle w_{,s}\quad\frac{1}{r}(\triangle w_{,\theta}-\triangle v)]^T,$$

$$\{\triangle q\}=\{\triangle u\quad\triangle v\quad\triangle w\}^T,$$

$$\{\sigma\}=[\sigma_s\quad\sigma_\theta\quad\tau_{s\theta}]^T,\quad\{\sigma\}_{st}=[0\quad\sigma_\theta\quad0]^T,$$

$$[S_0]=\begin{pmatrix}\sigma_s&\tau_{s\theta}\\\tau_{s\theta}&\sigma_\theta\end{pmatrix},\quad[S_0]_{st}=\begin{pmatrix}0&0\\0&\sigma_\theta\end{pmatrix}$$

and subscript 'st' refers to ring-stiffeners.

3. Finite Element Formulation for Ultimate Strength Analysis

In order to perform a one-dimensional finite element analysis of a circular cylinder, the cylinder was longitudinally discretized into a number of axisymmetric shell elements and the displacement field within each element was assumed to consist of two sets of components; an axisymmetric component (u_0, w_0) and an asymmetric one (u_1, v_1, w_1) and expressed(Subbiah, 1988) as

$$\begin{aligned}&u_0=a_1+a_2\xi,\quad w_0=a_3+a_4\xi+a_5\xi^2+a_6\xi^3\\&u_1=(a_7+a_8\xi)\cos j\theta,\quad v_1=(a_9+a_{10}\xi)\sin j\theta\\&w_1=(a_{11}+a_{12}\xi+a_{13}\xi^2+a_{14}\xi^3)\cos j\theta\end{aligned} \tag{11}$$

The 14 constants $(a_1, a_2, \cdots, a_{14})$ in the above equation are related to the nodal displacement degrees of freedom $\{d^e\}$ and thus the displacement field can be written in terms of $\{d^e\}$ as

$$\{q\}=[N]\{d^e\} \tag{12}$$

where $\{q\}=[u_0+u_1\ v_1\ w_0+w_1]^T$, $\{d^e\}=[u_{0i}\ w_{0i}\ \beta_{0i}\ u_{1i}\ v_{1i}\ w_{1i}\ \beta_{1i}\ u_{0j}\ w_{0j}\ \beta_{0j}\ u_{1j}\ v_{1j}\ w_{1j}\ \beta_{1j}]$ and $[N]$ is a 3 x 14 shape function matrix. Eq. (12) can be written in an incremental form as

$$\{\triangle q\}=[N]\{\triangle d^e\} \tag{13}$$

Incremental strain expressed as eq. (4) can be expressed in terms of $\{\triangle d^e\}$ as

$$\{\triangle\varepsilon\}=[B]\{\triangle d^e\}=([B_m]+[B_n])-z[B_b])\{\triangle d^e\} \tag{14}$$

Then $\{\triangle\phi\}$ in eq. (10), $\{d_{f1}\}$ and $\{d_{f2}\}$ in eq. (9) can, respectively, be expressed as

$$\begin{aligned}&\{\triangle\phi\}=[A]\{\triangle d^e\},\\&\{d_{f1}\}=[B_{f1}]\{d^e\},\quad\{d_{f2}\}=[B_{f2}]\{d^e\}\end{aligned} \tag{15}$$

3.1 Construction of the elasto-plastic stiffness matrix

By putting eqs. (13)-(15) into eq. (10) and dividing both sides of the equation by $\delta\{\triangle d^e\}^T$ since the virtual work equation should be valid for any virtual displacement, an incremental equilibrium equation is obtained and can be written in a simple form as

$$[K][\triangle d]-\{\triangle F^e\}=\{R\} \tag{16}$$

where $\{\triangle d\}$ is the nodal displacement increment vector for the total structure, $\{\triangle F^e\}$ is the equivalent nodal force increment vector, $\{R\}$ is the residual force vector and $\{K\}$ is the total stiffness matrix expressed as

$$\begin{aligned}[K]=\sum^{EL}&([k_{mm}]_{sh}+[k_{mb}]_{sh}+[k_{bm}]_{sh}\\&+[k_{bb}]_{sh}+[k_G]_{sh}+[k_{mm}]_{st}+[k_{mb}]_{st}\\&+[k_{bm}]_{st}+[k_{bb}]_{st}+[k_G]_{st})\end{aligned} \tag{17}$$

where

$$\begin{aligned}&[k_{mm}]=\int_v[B_m]^T[D][B_m]dv^e\\&[k_{bm}]=[k_{bm}]^T=\int_v[B_m]^T[D]([B_n]-z[B_b])dv^e\\&[k_{bb}]=\int_v[B_n]^T[D][B_n]-z([B_n]^T[D][B_b]\\&\qquad+[B_b]^T[D][B_n])+z^2[B_b]^T[D][B_b])dv^e\end{aligned} \tag{18}$$

$[k_G]=\int_v [A]^T[S_0][A]dv^e$: initial stress matrix

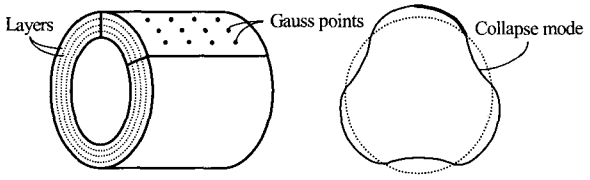

Fig. 2 Arrangement of Gauss points and layers over an element

As eq. (18) shows, the construction of element stiffness matrices requires the volume integration of specified forms of [B][D][B] which cannot be analytically integrated to the circumferential direction except when [D] is a constant matrix prior to the initial yielding. However, it is essential to perform the circumferential integration without generating meshes to the circumferential direction for making one-dimensional axisymmetric ultimate strength analysis possible. In order to solve this problem, this paper introduced Gauss quadruture to the circumferential integration as well as to the longitudinal one within an axisymmetric shell element, which excludes the necessity of the whole cylinder to be meshed to the circumferential direction and makes one-dimensional analysis possible. Fig. 2 shows an example of Gauss point layout for a numerical integration both to the circumferential and the longitudinal directions within an element. Besides, circumferential integration can be performed only for the quarter wave length of an assumed collapse mode in order to enhance the calculation efficiency using periodicity. Thickness integration is performed by applying the trapezoidal rule to the layered shell.

3.2 Solution procedure for the nonlinear problem

Combined load-increment and iteration procedure was used to solve the incremental equilibrium equation expressed as eq. (16).

First, initial imperfections were assumed as the starting point of total displacement and initial stress vectors, then the stiffness matrix and the load increment vector were determined using the present displacement and initial stress vectors. Then the matrix equation was solved to obtain the displacement increment vector to be accumulated upon the present displacement. After that, the residual force vector was calculated and used as a load vector for the next iteration stage. This iteration continued until the convergence was satisfied by the convergence criteria that the ratio of residual force norm and incremental force norm should reach a certain tolerance level (here taken as 0.005). Once the convergence is satisfied, iterations were stopped and the next load-incremental step was followed. In the meanwhile, when the accumulated load reached the ultimate strength point, the norm ratio became larger as iteration continues and the calculation was to diverge. The program is designed to stop the calculation there and to take the last accumulated load as the ultimate strength value.

4. Initial Imperfections

Initial imperfections inevitably involved in the process of fabrication are composed of initial deformations and initial stresses.

4.1 Initial deformations

The general shape of initial deformations can be expressed by a double Fourier series, being divided into two parts, as follows (Kenny, 1984)

$$w_1(s,\theta)=\sum_i A_{oi}\cos\frac{i\pi s}{L}+\sum_n\sum_k A_{kn}\cos\frac{k\pi s}{L}\cos n\theta \qquad (19)$$

In the above equation the first and the second parts respectively represent the axisymmetric and non-symmetric parts. In this paper, however, only the non-symmetric part of the shape imperfection is taken under the assumption that the ultimate strength of ring-stiffened circular cylinders is mostly affected by the non-symmetric collapse [or buckling] mode of the cylinder. In addition, for the sake of calculation efficiency, each term of the non-symmetric series (2nd part of eq. (19)) is individually applied and divided into two categories in order to take into account both the collapse modes; interframe shell collapse and general collapse of a ring-stiffened cylinder. Accordingly, the following two cases are considered as initial deformations (Subbiah, 1988).

$w_1'=e\sin\frac{\pi s}{l}\cos n\theta$ for interframe shell collapse,

$w_1'=e\sin\frac{\pi s}{L}\cos n\theta$ for the general collapse

where e, n, l and L are the amplitude of shape imperfection, the number of circumferential waves of collapse mode, ring-stiffener space and overall length of the cylinder, respectively.

4.2 Initial stresses

While a ring-stiffened cylinder may have a variety of initial stresses depending on the fabrication process, this paper has taken into account only two typical types of circumferential stresses and their combinations, which are respectively named 'first-type initial stress' , 'second-type initial stress' and 'combined initial stress'.

4.2.1 First-type initial stress

This refers to the initial stress generated due to the cold-bending of steel plates. It has a distribution which varies over the thickness of a shell as shown in Fig. 3 keeping uniform over the surface.

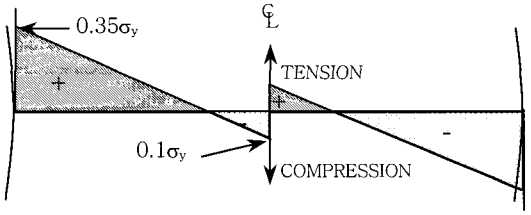

Fig. 3 Circumferential initial stress distribution of fabricated tubes due to cold-bending (Kenny, 1984)

4.2.2 Second-type initial stress

This refers to the initial stress generated by the welding of ring-stiffeners to the cylinder. As shown in Fig. 4, it does not vary over the thickness of the shell but has different uniform values in two regions. The banded region within a certain distance (ηt; t denotes the thickness of the shell) on both sides from each ring-stiffener has the value of tensile yield stress and the rest has compressive stress to equilibrate the tensile stress (Kenny, 1984). While η is experimentally known as having a value between 3 and 6 (Hughes,1983), 4 is adopted for the present calculation.

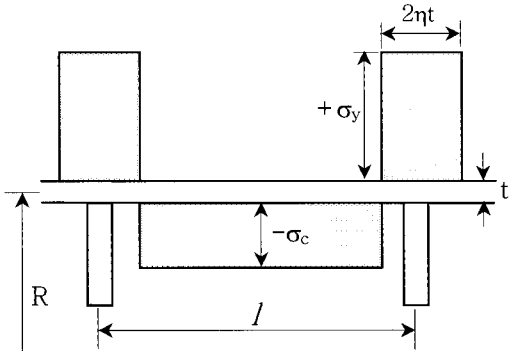

Fig. 4 Circumferential residual stress due to the welding of ring-stiffeners to the cylinder

5. Numerical Analysis and Investigation

While the present ultimate strength analysis method has been developed to cover the whole range of ratios of axial and lateral pressures, a numerical analysis was conducted only for the case of hydrostatic pressure.

5.1 Validity check for the developed method

Cho et al. (2000) have manufactured and tested several ring-stiffened cylinders under hydrostatic pressure loads. This paper has chosen one of them as our analysis model. The dimensions and scantlings are shown in Fig. 5 and Table 1. In order to check the validity of our developed method, it and two widely -used commercial codes (NASTRAN and ABAQUS) were simultaneously applied to the chosen model, and the results are shown in Table 2 to be compared.

Table 2 shows some differences even between the results of two widely-used commercial codes and our present method is thought to give satisfactory results showing no significant difference between the results of the two commercial codes.

Table 1 Geometrical and material property of the model (RS-2)

Shell	Diameter(mm)	542.0
	Thickness(mm)	2.27
	Spacing of mid-bay(mm)	80.0
	Yield stress(N/mm^2)	310.8
	Young's modulus(N/mm^2)	217300
Ring-stiffener	No. of stiffeners	4
	Height(mm)	25.0
	Thickness(mm)	3.88
	Yield stress(N/mm^2)	297.5
	Young's modulus(N/mm^2)	205300
Length overall(mm)	340	

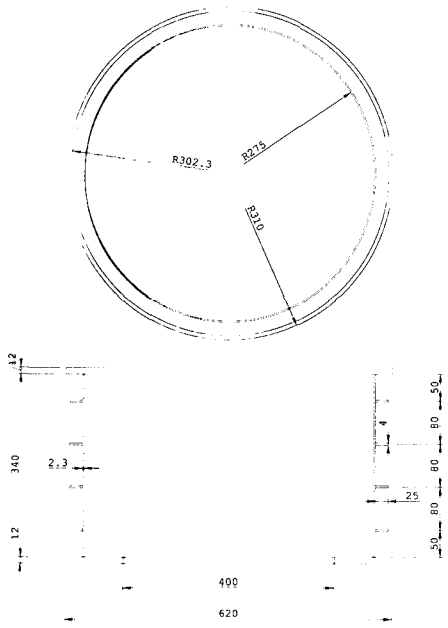

Fig. 5 Analysis model (RS-2)

Table 2 Comparison of ultimate strength for two cases; with and without initial stresses (unit; N/mm^2)

Initial deflection (w_1)	Without initial stresses		
	NASTRAN	ABAQUS	Present method
0.000R	2.244	2.098	2.20
0.001R	1.812	1.796	1.78
0.002R	1.493	1.503	1.56
0.003R	1.340	1.368	1.48

Initial deflection (w_1)	With 2nd type initial stresses		Ultimate strength reduction(%) due to initial stress	
	ABAQUS	Present method	ABAQUS	Present method
0.000R	2.052	2.06	2.2%	6.4%
0.001R	1.678	1.69	6.6%	5.1%
0.002R	1.403	1.46	7.0%	6.4%
0.003R	1.264	1.39	7.6%	6.1%

5.2 Imperfection sensitivity of ultimate strength

In order to perform parametric studies for the effect of initial imperfections on ultimate strength, 9 models were set up to cover a variety of geometric properties ranging 3 steps of length-thickness ratio; (A), (B), (C) and 3 steps of radius-thickness ratio; (1), (2), (3). Each of the models is constructed by combining these two series, as shown in Table 3. Table 4 shows the geometrical and material properties of all the calculated models. Each model was analyzed for various values of initial deformation and for four cases of initial stresses like no initial stress, first-type initial stress, second-type initial stress and combined initial stress. Calculated results are arranged in 9 Tables; Table 5 through 13. Following are observations from the calculated results.

- Ultimate strength reductions due to first-type initial stress shows little variation from model to model and generally remains under the small value of 2%.
- Ultimate strength reductions due to second-type initial stress are large in the order of (A), (B), (C), that is, larger as the ratio of ring space to shell thickness is smaller.
- Ultimate strength reductions due to combined initial stress show little characteristic relations with the geometrical properties of the models remaining between 5 to 8%.

Table 3 Calculated models for parametric study

L_r/t / R/t	(A) 15	(B) 30	(C) 45
(1) 30	A1	B1	C1
(2) 60	A2	B2	C2
(3) 90	A3	B3	C3

Table 4 Geometric and material properties of the calculated models

Model	L_r (mm)	R (mm)	t (mm)	L_r/t	R/t	E [GPa]	σ_y [MPa]
A1	80	160	5.33	15	30	204	272
A2	80	320	5.33	15	60	204	272
A3	80	480	5.33	15	90	204	272
B1	80	80	2.67	30	30	204	272
B2	80	160	2.67	30	60	204	272
B3	80	240	2.67	30	90	204	272
C1	80	53.33	1.78	45	30	204	272
C2	80	106.66	1.78	45	60	204	272
C3	80	160	1.78	45	90	204	272

Table 5 Ultimate strength variations of A1 model due to initial imperfections (No. of circumferential wave= 7, unit; N/mm^2)

Initial deflection (w_1)	No initial stress	1st type initial stress	2nd type initial stress	combined initial stress
0.000R	12.65	12.60(0.4%)	10.15(19.8%)	12.20(3.6%)
0.001R	12.60	12.55(0.4%)	9.85(21.8%)	11.30(5.0%)
0.002R	12.40	12.35(0.4%)	9.65(22.2%)	11.80(4.8%)
0.003R	12.15	12.05(0.8%)	9.55(21.4%)	11.55(4.9%)
0.004R	11.85	11.75(0.8%)	9.25(21.9%)	11.25(5.1%)
0.005R	11.55	11.45(0.9%)	9.00(22.1%)	10.95(5.2%)

Table 6 Ultimate strength variations of A2 model due to initial imperfections (No. of circumferential wave= 8, unit; N/mm^2)

Initial deflection (w_1)	No initial stress	1st type initial stress	2nd type initial stress	combined initial stress
0.000R	7.20	7.10(1.4%)	6.95(3.5%)	6.95(3.5%)
0.001R	6.65	6.50(0.8%)	6.25(6.0%)	6.30(5.3%)
0.002R	6.60	6.50(1.5%)	5.95(9.8%)	6.30(4.8%)
0.003R	6.30	6.20(1.6%)	5.55(11.9%)	6.05(4.0%)
0.004R	6.05	6.00(0.8%)	5.30(10.7%)	5.85(3.3%)
0.005R	5.85	5.80(0.9%)	5.65(3.4%)	5.65(3.4%)

Table 7 Ultimate strength variations of A3 model due to initial imperfections (No. of circumferential wave= 10, unit; N/mm^2)

Initial deflection (w_1)	No initial stress	1st type initial stress	2nd type initial stress	combined initial stress
0.000R	5.15	5.08(1.4%)	4.90(4.9%)	5.04(2.1%)
0.001R	4.76	4.70(1.3%)	4.46(6.3%)	4.60(3.4%)
0.002R	4.44	4.40(0.9%)	4.06(8.6%)	4.22(5.0%)
0.003R	4.22	4.18(0.9%)	3.80(10.0%)	4.08(3.3%)
0.004R	4.04	4.00(1.0%)	3.70(8.4%)	3.92(3.0%)
0.005R	3.90	3.88(0.5%)	3.80(2.6%)	3.80(2.6%)

Table 8 Ultimate strength variations of B1 model due to initial imperfections (No. of circumferential wave= 8, unit; N/mm^2)

Initial deflection (w_1)	No initial stress	1st type initial stress	2nd type initial stress	combined initial stress
0.000R	10.65	10.65(0.0%)	9.95(6.6%)	9.95(6.6%)
0.001R	10.00	9.95(0.5%)	9.60(4.0%)	9.45(5.5%)
0.002R	9.60	9.55(0.5%)	9.20(4.2%)	9.00(6.3%)
0.003R	9.20	9.10(1.1%)	8.75(4.9%)	8.55(7.1%)
0.004R	8.80	8.70(1.1%)	8.55(2.8%)	8.15(7.4%)
0.005R	8.40	8.35(0.6%)	8.15(3.0%)	8.05(4.2%)

Table 9 Ultimate strength variations of B2 model due to initial imperfections (No. of circumferential wave= 10, unit; N/mm^2)

Initial deflection (w_1)	No initial stress	1st type initial stress	2nd type initial stress	combined initial stress
0.000R	5.40	5.38(0.4%)	4.96(8.1%)	4.98(7.8%)
0.001R	4.88	4.82(1.2%)	4.56(6.6%)	4.58(6.1%)
0.002R	4.48	4.44(0.9%)	4.34(3.1%)	4.26(4.9%)
0.003R	4.16	4.12(1.0%)	4.02(3.4%)	3.96(4.8%)
0.004R	3.92	3.90(0.5%)	3.78(3.6%)	3.74(4.6%)
0.005R	3.76	3.74(0.5%)	3.64(3.2%)	3.62(3.7%)

Table 10 Ultimate strength variations of B3 model due to initial imperfections (No. of circumferential wave= 11, unit; N/mm^2)

Initial deflecti-on(w_1)	No initial stress	1st type initial stress	2nd type initial stress	combined initial stress
0.000R	3.66	3.62(1.1%)	3.48(4.9%)	3.54(3.3%)
0.001R	3.18	3.14(1.3%)	3.12(1.9%)	3.04(4.4%)
0.002R	2.88	2.84(1.4%)	2.82(2.1%)	2.74(4.9%)
0.003R	2.70	2.68(0.7%)	2.62(3.0%)	2.58(4.4%)
0.004R	2.58	2.56(0.8%)	2.54(1.6%)	2.52(2.3%)
0.005R	2.56	2.54(0.8%)	2.52(1.6%)	2.50(2.3%)

Table 11 Ultimate strength variations of C1 model due to initial imperfections (No. of circumferential wave= 6, unit; N/mm^2)

Initial deflecti-on(w_1)	No initial stress	1st type initial stress	2nd type initial stress	combined initial stress
0.000R	10.30	10.30(0.0%)	10.10(1.9%)	10.00(2.9%)
0.001R	9.60	9.50(1.0%)	9.50(1.0%)	9.10(5.2%)
0.002R	8.90	8.85(0.6%)	8.85(0.6%)	8.35(6.2%)
0.003R	8.35	8.30(0.6%)	8.30(0.6%)	8.05(3.6%)
0.004R	7.85	7.80(0.6%)	7.80(0.6%)	7.55(3.8%)
0.005R	7.40	7.35(0.7%)	7.35(0.7%)	7.15(3.4%)

Table 12 Ultimate strength variations of C2 model due to initial imperfections (No. of circumferential wave= 9, unit; N/mm^2)

Initial deflection (w_1)	No initial stress	1st type initial stress	2nd type initial stress	combined initial stress
0.000R	5.16	5.16(0.0%)	5.12(0.8%)	4.84(6.2%)
0.001R	4.24	4.18(1.4%)	4.20(0.9%)	3.94(7.0%)
0.002R	3.72	3.68(1.1%)	3.68(1.1%)	3.54(4.8%)
0.003R	3.38	3.36(0.6%)	3.34(1.2%)	3.22(4.7%)
0.004R	3.16	3.10(1.9%)	3.10(1.9%)	3.02(4.4%)
0.005R	3.02	2.98(1.3%)	2.96(2.0%)	2.92(3.3%)

Table 13 Ultimate strength variations of C3 model due to initial imperfections (No. of circumferential wave= 11, unit; N/mm^2)

Initial deflection (w_1)	No initial stress	1st type initial stress	2nd type initial stress	combined initial stress
0.000R	3.42	3.40(0.6%)	3.40(0.6%)	3.38(1.2%)
0.001R	2.54	2.51(1.2%)	2.52(0.8%)	2.40(5.5%)
0.002R	2.22	2.20(0.9%)	2.18(1.8%)	2.10(5.4%)
0.003R	2.06	2.04(1.0%)	2.02(1.9%)	2.00(2.9%)
0.004R	2.00	1.98(1.0%)	1.96(2.0%)	1.94(3.0%)
0.005R	1.98	1.96(1.0%)	1.94(2.0%)	1.93(2.5%)

6. Conclusions

This paper has developed an one-dimensional finite element method which is efficient in terms of time consumption while covering any form of initial imperfections. Our developed method proved to be valid by showing its results in good agreement with the results from MSC/NASTRAN and HKS/ABAQUS. It was then used for parametric studies to investigate the imperfection sensitivity of the ultimate strength of ring-stiffened cylinders. This study shows that initial stress sensitivity is strongly affected by the geometrical properties of a cylinder and generally not negligible although it is less remarkable than initial deformation sensitivity.

Aknowledgements

This paper is supported by the research fund 2002 of the University of Ulsan.

References

Brush, D.O. and Almroth, B.O. (1975). Buckling of Bars, Plates and Shells, McGraw-Hill, pp 147.

Cho, S.R., Kim, S.M. and Kim, H.J. (2000). "Experimental Investigation on the Ultimate Strength of Ring-Stiffened Cylinders", Transactions of the Korea Ship and Offshore Structures Congress, Vol 14, No 1, pp 1-8

Hughes, O.F. (1983). Ship Structural Design; A Rationally-Based, Computer-Aided, Optimization Approach, John Wiley & Sons.

Kenny, J.P. (1984). Buckling of Offshore Structure, GULF, pp 23-152.

Owen, D.R.J. and Hinton, E. (1980). Finite Elements in Plasticity : Theory and Practice, Pineridge Press Ltd., pp 224-228.

Park, C.M. (1990). Ultimate Strength Analysis of Ring-stiffened Circular Cylindrical Shells, Ph.D. Thesis at Seoul National University, Korea, pp 29-32.

Park, C.M. and Lee, S.H. (2001). "Ultimate Strength Analysis of Ring-Stiffened Cylinders Using Commercial Softwares(I)", Journal of Ocean Engineering and Technology, Vol 15, No 2, pp 120-123.

Park, C.M. and Lee, S.H. (2002). "Ultimate Strength Analysis of Ring-Stiffened Cylinders Using Commercial Softwares(II)", Journal of Ocean Engineering and Technology, Vol 16, No 1, pp 36-40.

Subbiah, J. and Natarajan, R. (1982). "Stability Analysis of Ring-Stiffened Shell of Revolution" , Journal of Ship Research, Vol 26, No 2, pp 125-134

Subbiah, J. (1988). "Nonlinear Analysis of Geometrically Imperfect Stiffened Shells of Revolution" , Journal of Ship Research, Vol 32, No 1, pp 74-83.

Washizu, K. (1975). Variational Methods in Elasticity and Plasticity , Pergamon Press.